Desalination and Water Treatment
www.deswater.com

doi: 10.1080/19443994.2013.838525

53 (2015) 66–72
January

Taylor & Francis
Taylor & Francis Group

Color, COD, and salt retention by inorganic membrane

K. Zaiter[a], A. Belouatek[a,*], A. Chougui[a], B. Asli[a], A. Szymczyk[b]

[a]*Laboratoire Environnement, les Substances Naturelles Végétales et Technologie des Aliments (E.S.N.T.A), Centre universitaire de Relizane, Relizane, Algeria*
Tel. +213 553031811; email: abelouatek@voila.fr
[b]*Université de Rennes 1, Institut des Sciences Chimiques de Rennes (UMR CNRS 6226), Rennes, France*

Received 19 April 2013; Accepted 6 August 2013

ABSTRACT

Ceramic membranes are now being developed as a new technology to treat polluted waters. Although inorganic membranes have replaced organic membranes in many industrial applications, they have yet to be used widely in desalination processes. In this paper, the retention of a series of dyes, wastewater, and salt molecules by two membranes (symbolized MLS and AMLS) was studied. Filtration tests were performed on a laboratory-scale filtration, using a recycling configuration at 5 bar. In the present study, the application of the filtration process is investigated mainly in the retention of color, heavy metals, and chemical oxygen demand (COD) present in wastewater. Filtration studies using ceramic membranes were performed for solutions containing salts, Congo red, lead ($Pb(NO_3)_2$), and industrial waste water. The results showed permeate flux for different wastewaters through these membranes varied from 274.28 $L/h\,m^2$ (for AMLS) to 514.29 $L/h\,m^2$ (for MLS). The rejection rate salts and Congo red were strongly influenced by the electrical interactions between ionic species and surface membrane. The maximum observed solute retention, using AMLS membrane, of lead ion, Congo red, and NaCl was 100%, 95%, and 47%, respectively. Cross-flow filtration was carried out then, in order to reduce the turbidity and COD. The result showed a high retention of turbidity (100%) and COD (87%).

Keywords: Ceramic membrane; Synthesis; COD; Dyes; Heavy metals and flux

1. Introduction

In recent years, water pollution with heavy metals and dyes has become an important environmental threat, mainly because of many industrial effluents containing these and other pollutants [1]. Heavy metals are highly toxic, non-biodegradable, and tend to accumulate causing several diseases and health disorders in humans, and other living organisms [2]. In particular, lead (Pb) has been classified as a serious hazardous heavy metal with high priority in the context of environmental risk [3]. This metal is extremely toxic and can damage the kidney, liver, brain, nervous, and reproductive systems among other adverse effects to humans [2]. At present, lead (Pb) pollution is considered a world-wide problem because this metal is commonly detected in several industrial wastewaters [1].

On the other hand, the removal of color from aquatic systems caused by the presence of synthetic dyes that usually contains azo-aromatic groups is extremely important from the environmental viewpoint

*Corresponding author.

because most of these dyes are toxic, mutagenic, and carcinogenic [4,5]. Congo red dye is one of the important azo dyes. It is a colored substance with complex chemical structure and high molecular weight. The chemical structure is the sodium salt of benzidinediazo-bis-1-naphtylamine-4-sulfonic acid. It is highly soluble in water and persistent in the environment, once discharged into a natural environment. Thus, the study on Congo red is interesting not only for being possible pollutants of industrial effluents, but also because it is a good model of complex pollutants [6].

Many methods are available for the removal of pollutants from water, the most important of which are biodegradation [7] and adsorption [8]. Recently, membrane separation technologies have been used for the separation of dyes and heavy metals [9,10].

Typically, porous ceramic membranes are asymmetric with a support thickness of about 1–3 mm. The microfiltration layer is usually 10–30 μm thick, and the most common oxides used for the membranes are zirconia (ZrO_2) and alumina (Al_2O_3). Ultrafiltration membranes are of few micrometers thick and typical materials are alumina, zirconia, titania (TiO_2), and ceria (CeO_2). Nanofiltration membranes are less than 1 μm thick, generally made of zirconia and titania. The support and the microfiltration layer are elaborated by classical ceramic techniques. The sol–gel process is used for ultrafiltration and nanofiltration layers [11–14].

The feed properties can be changed by pretreatments such as pH adjustment, thermal treatment, addition of chemicals, and pre-filtration. The pH adjustment [15] and thermal treatment can decrease the precipitation of certain substances and thus the fouling of the membrane. The salt concentration of the feed and the valence of the salt present can also be important [16–18].

The goal of this work is to study the filtration of the polluting substances (Congo red (CR), lead (Pb), salts, and industrial waste) from aqueous solution by a new type of ceramic membrane prepared from Algerian kaolin mixed with a percentage of ZrO_2 and coated with thin layer of alkoxide (TEOS).

2. Materials and methods

We developed and prepared in the laboratory two different types of membranes: a support made up of a mixture of local kaolin (Algerian kaolin) and percentage of zirconia (3% ZrO_2 in weight) symbolized by MLS; to improve the membrane performance, we added a thin layer of alkoxide (TEOS) on the support MLS. So the ceramic membrane AMLS has the same structure of the first, and second layer is prepared via a sol–gel technique from colloidal suspensions synthesized by TEOS (tetraethylorthosilicate) and alcohol followed by peptization under acidic conditions. The slip-casting procedure is followed by drying and calcination at temperature 780˚C. The tests of filtration were carried out on these membranes, the characteristics of which were the following: length = 300 mm; internal–external diameter = 13/16 mm/mm. The flow chart of the pilot used is represented in Fig. 1. Filtration was of tangential type and the pressure applied was 5 bar.

The morphology and microstructure of MLS membrane were characterized by a scanning electron microscope. Phases present in the mixture of kaolin and 3% ZrO_2 (raw powder and heated to 1,150˚C) were analyzed using an X-ray diffractometer (Siemens, Germany) with Cu Kα1 radiation ($\lambda = 1{,}54{,}056$ Å).

The thermogravimetric analysis (TGA) and differential scanning calorimetry (DSC) of the MLS membrane were carried out at the temperature ranging between 0 and 1,000˚C at a rate of 5˚C/min under air.

The performances of MLS and AMLS membranes were mainly described by water flux (F) and rejection rate (TR%) of solutions. Filtration was of tangential type and the pressure applied was 5 bar.

The salt rejection of these membranes is tested by filtering two different salt solutions, $MgCl_2$ and NaCl, prepared at a concentration of 1,000 ppm and a pH range from 5.8 to 6.2. Permeate analysis of the saline solution was carried out by conductimetry (model DDSJ-308A).

Dissolved salts concentration is directly related to conductivity by the following relationship:

$$K = \gamma \times \Lambda c \times C \quad (1)$$

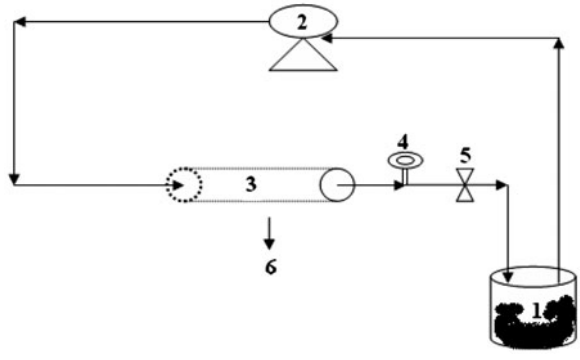

Fig. 1. Filtration flow diagram [17,18].
(1) Feed tank; (2) feed pump; (3) tubular membrane; (4) manometer; (5) pressure valve; and (6) filtrate recover.

where K is the specific conductivity, γ is the conversion factor, Λc is the molar conductivity, and C is the molar concentration of salt.

Hence, measuring the filtrate conductivity allows the determination of the corresponding saline concentration providing a standardizing procedure beforehand $K = f(c)$. The percent retention was calculated by equation (2).

$$\mathrm{TR}(\%) = 1 - \frac{C_{sp}}{C_{sa}} \quad (2)$$

Permeate and feed analysis of the colored solution were measured by visible spectrophotometry (optizen 120 UV), while the heavy metal (lead) solution was carried out by an atomic emission spectrometer (Aurora AI 1200).

The chemical oxygen demand (COD) retention rate (COD industrial waste) IS determined by dichromate of potassium method. The characteristics of various solutes available in the solution are presented in Table 1.

For the experiments reproducibility, we have repeated the experiments three times for all the results and we agree this value when the variance coefficient (CV) is less 5%.

3. Results and discussion

3.1. Characterization of membranes

3.1.1. Thermal analysis

Structural evolution of the powder evaluated by thermogravimetric analysis (TGA) and differential scanning calorimetry (DSC) analysis show the weight loss of kaolin + 3 wt.% ZrO_2 mixtures (MLS). These two analyses have been carried out under air. The heating rate of the compacts from room temperature to 1,000°C was 5°C/min, while the cooling of compacts was carried out in the furnace.

Table 1
Characteristics of rejects liquid effluent

Effluent	Conductivity (μS/cm)	pH	DCO (mg O_2/L)
(BCR) factory reject	1,534	7.19	302
(Hydro-canal) factory reject	2,480	9.87	244
(SOAChlore) factory reject	4,760	7.78	176
Urban rejects	1,833	7.71	816

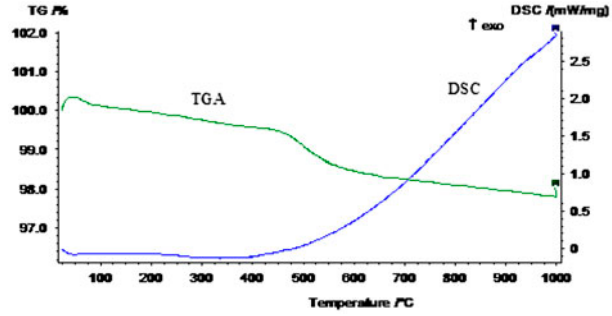

Fig. 2. Thermal analysis curve: DSC and TGA for MLS support.

TGA curves recorded during compacts heating (Fig. 2) permit the following remarks of a total weight loss of about 2.4% of MLS compacts is measured. In fact, this weight loss consists of two distinct stages. The first one is attributed to the humidity (water added into the starting mixtures), whereas the second stage is related to the departure of water (by vaporization) existing in the kaolin chemical composition. The weight loss ratio of the last stage is more pronounced (Fig. 2).

A further weight loss is observed during MLS compacts heating. This weight loss is mainly due to kaolin rehydration [19–21] from $Al_2Si_2O_5(OH)_4$ to Al_2O_3 $2SiO_2$. This rehydration is characterized by one additional peak (Fig. 2) appearing at about 980°C.

These observations are also confirmed by DSC analysis. The endothermic phenomena, appearing at 65 and 480°C, correspond to the first and the second stages of weight loss, respectively, some workers attribute this reaction to spinel formation while others attribute it to mullite nucleation [22]. More possibly, this reaction may be attributed to mullite nucleation, since XRD shows that mullite nucleates first at a relatively lower temperature, before spinel nucleation.

3.1.2. Phase identification

X-ray diffraction was used to identify the formed phases. For kaolin mixed with 3 wt.% ZrO_2 (MLS), the main observed phases are: kaolinite (K), muscovite (M), and quartz (Q) as shown in Fig. 3(a). However, for samples sintered at 1,150°C, the kaolinite phase disappeared Fig. 3(b). It shows that mullite phase (M) is the main crystalline mineral present in this powder, and zirconia (monoclinic system) was detected as a minor phase. Moreover, this means that the porosity is independent of the formed phases. These identified phases are of great importance because of their promising physical and mechanical properties.

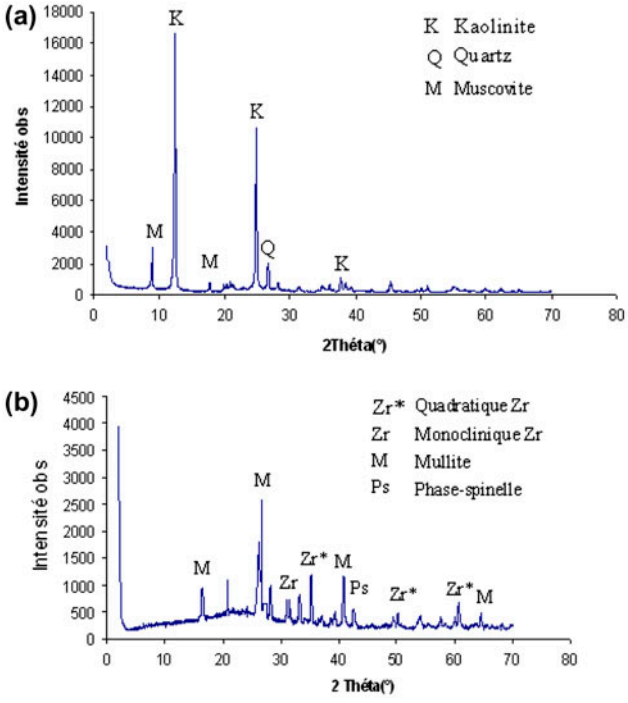

Fig. 3. X-ray diffractogram of the mixture of kaolin and 3% ZrO_2 (a) raw powder; (b) heated to 1,150°C.

3.1.2.1. Microstructures. The microstructure morphology for the surface and the cross-section of a MLS support are shown in Fig. 4. This figure gives information on the texture of the elaborated membrane surface. A defect free membrane was only obtained for the membrane which has low thickness. Evidently, the porous structure derived from the pore former is much more obvious in Fig. 4(b). The open paths and channels among pores, derived from higher connectivity, result in an open porosity.

3.1.2.2. Porosity. The porosity of the MLS and AMLS membranes is approximately 26% and 32%, respectively. The pore size of the AMLS layer was 10 nm. The filtration area of the membranes varied from 0.012 to 0.0123 m^2 and the specific area of AMLS and MLS, express in m^2 filtration area/m^3 membrane volume, are 316 and 305, respectively.

3.2. Filtration tests

3.2.1. Permeability

Permeability of the membrane was measured to evaluate the integrity and the properties of the membrane (Fig. 5). In this figure, it clearly shows the permeability of the MLS membrane with just one layer was determined to be (220 L/h m^2) at 2 bar and (820L/h m^2) at 6 bar, but the permeability of the AMLS double layer membrane reveal the 75.9 L/h m^2 at 2 bar increase to 340 L/h m^2 at 6 bar. The result showed that depositing the top layer on the intermediate one has a small effect on the permeability of the double layer membrane, and the membrane permeation is reduced by a small amount. The lower water permeability of the multilayer membrane is explained by a smaller pore size and hydraulic conductivity when we applied an identical pressure.

The average following of the flux as a function of time for water at 5 bar for 2 h are presented in Fig. 6.

This figure shows the water flux of MLS membrane has the highest permeability around 587.76 L/h m^2 initially to reach a value of 489.22 L/h m^2. On the other, the AMLS membrane has lower permeation flux of 284.02 L/h m^2 decreased to 122.46 L/h m^2 due to the fouling of the membrane.

3.2.2. Retention rate

3.2.2.1. Salt rejection. Fig. 7 illustrates the salt rejections and permeation fluxes of the two negatively charged membranes. The AMLS has permeability around 274.28 L/h m^2 and the MLS has a higher permeability at 514.29 L/h m^2. The AMLS membrane

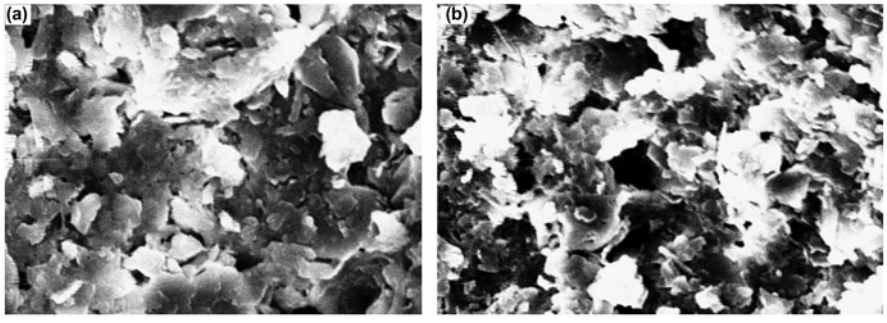

Fig. 4. Scanning electron microscopy of the support MLS (a) surface; (b) cross-section.

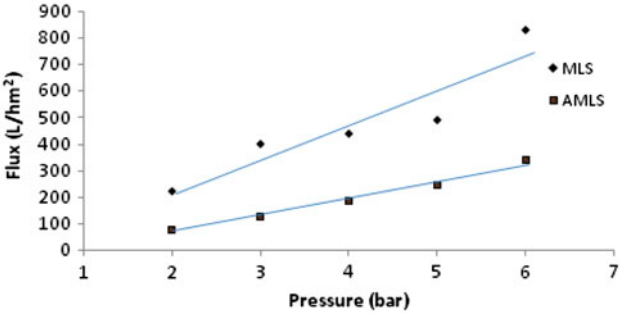

Fig. 5. Flux of water permeates vs. the pressures of MLS and AMLS membrane.

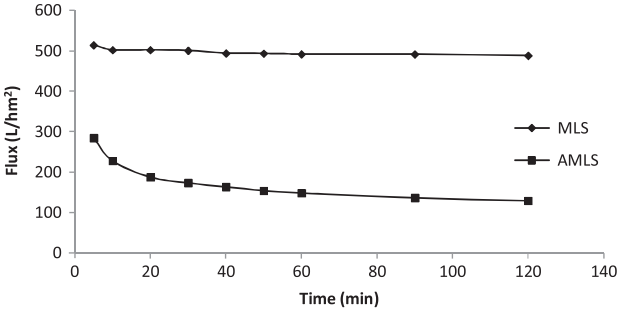

Fig. 6. Water flux as a function of time using MLS and AMLS membrane.

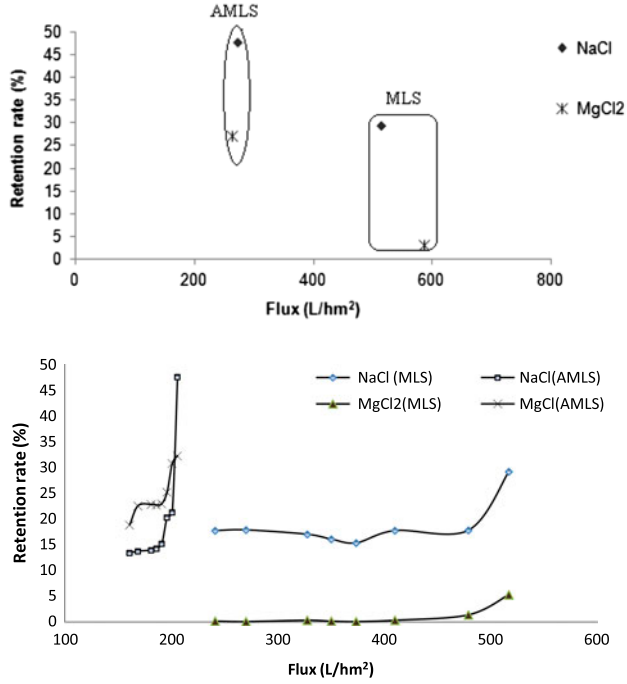

Fig. 7. The salt rejection and filtrate fluxes of membranes MLS and AMLS.

has the higher salt rejections than the MLS membrane does. We observe the AMLS membrane has a NaCl rejection as high as 47.58% and the MLS support has a NaCl rejection attained at 29.2%. Based upon the salt rejection, results of these two membranes follow the order: NaCl > $MgCl_2$ using MLS or AMLS membrane.

Membrane surface charge and Donnan exclusion can be used to account for the observed trend in the inorganic salt rejection. Since the active separating layer for AMLS membrane is composed of silica, the point of zero charge is three [25,26]. At a typical operating of a pH range from 5.8 to 6.2, the surface charge is negative.

Both of them belong to the type membrane defined by Schaep et al. [23]. Donnan exclusion dominates the separation and steric exclusion also affects the rejection. The negative charges on membranes reject preferably anions of the higher valence, which results in a higher rejection to chloride salts. The narrow passage in the separating layer of the membranes imposes stronger steric hindrance to the larger hydrated counter-ions, which results in a higher rejection to magnesium than sodium salts. It is difficult to imagine that the existence of strong steric hindrance in a membrane having pores of this size in micrometer [24,27].

The special character is their relatively high salt rejection. No matter the feed solution contains monovalent or divalent cations. The negatively charged membrane usually has a higher rejection towards NaCl. But, we observed the NaCl rejection using MLS membrane is still lower than that of the AMLS membrane (Fig. 7). However, the lower charge density of the counter ion accounts for the superior rejection of NaCl over the $MgCl_2$. In this case, the anion is shielded more effectively from the negatively charged surface by the polyvalent cation, yielding the observed trend in the rejection.

This is due to an electrostatic exclusion. The higher salt rejections defined by Peeters et al. [27]:

- Concentration in solution (and thus the salt concentration) is low.
- The charge density of the membrane is high.
- The valence of the co-ion is important.
- The valence of contre-ions is low.

3.2.2.2. Retention rate of Congo red. The MLS and AMLS membranes were evaluated by analyzing the rejection rate of the 10^{-4} M colored solutions of Congo red (molecular weight MW = 364.91 g/mol; pH = 6.46; λmax (nm) = 495).

The results show that the Congo red solution has high rejection rate. The latter depend on membrane

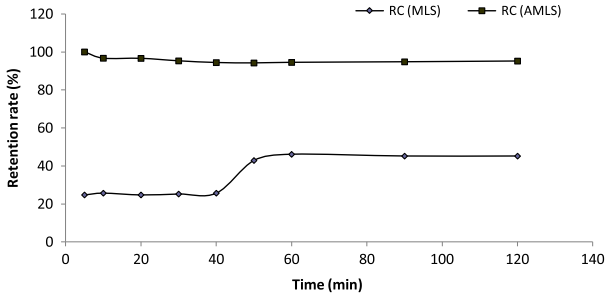

Fig. 8. Retention rate of Congo red solutions (10^{-4}M) vs. time of the MLS and AMLS membrane.

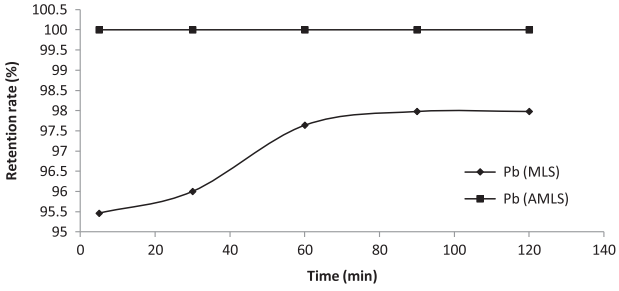

Fig. 9. Retention rate of lead (Pb) vs. time of the MLS and AMLS membrane.

pore diameter, interaction between solute ions and material charges, and solute molecular weight. It is illustrated in (Fig. 8) that the retention rate of MLS membrane attained is 24.74% in 30 min of treatment and increases gradually to value of 46%. In first step, before 50 min the retention rate of MLS is less because the pore size is important and after 50 min the pore size decreases by fouling phenomenon and the retention rate gets increased.

Using the AMLS membrane, the maximum retention of Congo red increased to 100% in 10 min, after the rate decreases to the value of 95%.

Table 2
Evolution of COD results vs. time of four effluents

Time (min)	COD (mg O_2 /L) (BCR) factory reject	Hydro-canal factory reject	SOAChlore factory reject	Urban reject
0	302	244	176	816
5	88	56	72	170
30	72	40	64	144
60	56	32	72	136
90	64	52	80	112
120	80	64	72	104

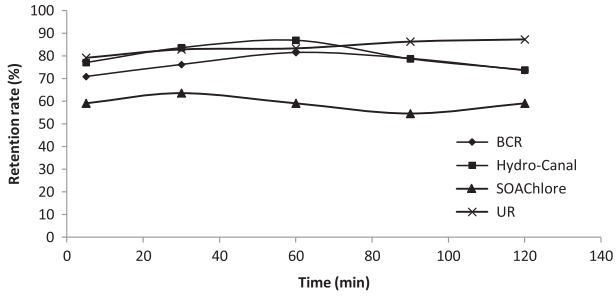

Fig. 10. Reduction of COD vs. time of the MLS membrane.

3.2.2.3. Removal of lead. The performance of the MLS and AMLS membrane, prepared in our laboratory for the retention of Pb^{2+}, under a pressure of 5 bar, from a 10^{-4} M solution concentration (at a pH of 5.8) is illustrated in Fig. 9.

The results show that the rejection rate of lead was in the range 95–97% using MLS membrane while the retention rate attained 100% using AMLS membrane. The removal of lead is mainly due to the strong interactions developed between the Pb^{2+} and the surface of the membrane.

3.2.2.4. COD reduction. Table 2 gives the evolution of COD of the raw and treated effluents. It can be noticed that the reduction of COD is very important (<120 mg O_2/L). Fig. 10 shows the retention rate of COD was higher than 59%. These results confirm the efficiency of these ultrafiltration-prepared membranes to liquid effluent treatment. However, this reduction of permeate COD increased to a value above the environmental norm of 120 mg O_2/L [28].

4. Conclusion

This study reports the development and the characterization of a new class of inorganic membrane containing a barrier layer. The AMLS membranes can be successfully applied for wastewater cleaning applications, as they exhibit significant salts, dye and metals retention efficiency by combining size and charge exclusion in a one-step process.

The results obtained with the membrane AMLS show that the membrane prepared can be applied to the treatment of liquid effluents. Efficiency of AMLS membrane for the liquid effluents treatment has been studied.

The flux of the AMLS membrane increased greatly as the operation pressure with constant rejection for dyes. Experiments show that the real rejection of Congo red and lead is in the range of 95–100% and depends on the membrane used, pressure, and

concentration of the feed. A membrane showed the best performance in terms of dyes and heavy metals removal and permeates flux.

These experimental results show that the MLS and AMLS material, for the development of ultrafiltration membranes, could be applied to the industrial wastewater treatment.

References

[1] S. Davydova, Heavy metals as toxicants in big cities, Microchem. J. 79 (2005) 133–136.

[2] H.A. Godwin, The biological chemistry of lead, Curr. Opin. Chem. Biol. 5 (2001) 223–227.

[3] B. Volesky, Detoxification of metal-bearing effluents: Biosorption for the next century, Hydrometall 59 (2001) 203–216.

[4] A.R. Gregory, S. Elliot, P. Kluge, Ames testing of direct black 3B parallel carcinogenicity, J. Appl. Toxicol. 1 (1991) 308–313.

[5] G. McKay, M.S. Otterburn, D.A. Aga, Fuller's earth and fired clay as adsorbent for dye stuffs. Equilibrium and rate constants, Water Air and Soil Pollut. 24 (1985) 307e22.

[6] T. Tapalad, A. Neramittagapong, S. Neramittagapong, M. Boonmee, Degradation of Congo red dye by ozonation, Chiang Mai J. Sci. 35(1) (2008) 63–68.

[7] G.M. Walker, L.R. Weatherley, Biodegradation and biosorption of acid anthraquinone dye, Environ. Pollut. 108 (2000) 219–223.

[8] S. Wang, Z.H. Zhu, A. Coomes, F. Haghseresht, G.Q. Lu, The physical and surface chemical characteristics of activated carbons and the adsorption of methylene blue from wastewater, J. Colloid Interface Sci. 284 (2005) 440–446.

[9] S. Chakraborty, S. De, J.K. Basu, S. DasGupta, Treatment of a textile effluent: Application of a combination method involving adsorption and nanofiltration, Desalination 174 (2005) 73–85.

[10] C. Fersi, L. Gzara, M. Dhahbi, Treatment of textile effluents by membrane technologies, Desalination 185 (2005) 399–409.

[11] A. Larbot, Ceramic processing techniques of support systems for membrane synthesis, in: A.J. Burggraaf, L. Cot (Eds.), Fundamentals of Inorganic Membrane Science and Technology, Elsevier Science B.V, Amsterdam, 1996, pp. 119–139.

[12] A. Larbot, C. Guizard, A. Julbe, L. Cot, Inorganic membranes: New concepts and developments, Membrane processes and applications, European Society of Membrane Science and Technology (ESMST) × Summer School on Membranes, September 20–24, 1993, Vallodolid, Spain, coordinador Antonio Hernández Giménez, Valladolid, Secretariado de Publicaciones, Universidad 199, pp. 27–39.

[13] C. Guizard, A. Ayral, A. Julbe, Present Status and New Developments of Ceramic Nanofiltration Membranes, 3rd Nanofiltration and Applications Workshop, Lappeenranta, Finland, 2001, 26–28.

[14] B.C. Bonekamp, Preparation of asymmetric ceramic membrane supports by dip coating, in: A.J. Burggraaf, L. Cot (Eds.), Fundamentals of Inorganic Membrane Science and Technology, Elsevier Science B.V, Amsterdam, 1996, pp. 141–225.

[15] P. Börgardts, W. Krischke, W. Trösch, H. Brunner, Integrated bioprocess for the simultaneous production of lactic acid and dairy sewage treatment, Bioprocess. Eng. 19(5) (1998) 321–329.

[16] S. Alami-Younssi, A. Larbot, M. Persin, J. Sarrazin, L. Cot, Gamma alumina nanofiltration membrane. Application to the rejection of metallic cations, J. Membr. Sci. 91 (1994) 87–95.

[17] A. Belouatek, A. Ouagued, M. Belhakem, A. Addou, Filtration performance of microporous ceramic supports, J. Biochem. Biophys. Methods 70 (2008) 1174–1179.

[18] A. Belouatek, N. Benderdouche, A. Addou, A. Ouagued, N. Bettahar, Preparation of inorganic supports for liquid waste treatment, J. Microporous Mesoporous Mater. 85 (2005) 163–168.

[19] G.W. Brindley, M. Nakahira, The kaolinite-mullite reaction series: I Survey of outstanding problems. II Metakaolin. III The high temperature phase, J. Am. Ceram. Soc. 42 (1959) 311–324.

[20] G.W. Brindley, J.H. Sharp, J.H. Patterson, A. Narshari, Kinetics and mechanism of dehydroxylation processes, Am. Mineral. 52 (1967) 201–211.

[21] R.R. Bhave, (Ed.), Inorganic Membranes: Synthesis, Characteristics and Applications, Van Nostrand Reinhold, New York, NY, 1991.

[22] A. Harabi, Studies of an alumina-chromia system containing mullite. PhD thesis, Manchester Materials Science Centre, UMIST, Manchester, 1990.

[23] J. Schaep, B.V.D. Bruggen, C. Vandecasteele, D. Wilms, Influence of ion size and charge in nanofiltration, Sep. Purif. Technol. 14 (1998) 155–162.

[24] B. Van der Bruggen, J. Schaep, D. Wilms, C. Vandecasteele, Influence of molecular size, polarity and charge on the retention of organic molecules by nanofiltration, J. Membr. Sci. 156 (1999) 29–41.

[25] C.L. Lin, D.L. Flowers, P.K.T. Liu, Characterization of ceramic membranes II, Modified commercial membranes with pore size under 4OA, J. Membr. Sci. 92 (1994) 45–58.

[26] H.P. Hsieh, Inorganic Membranes for Separation and Reaction, Membrane Science and Technology Series, 3, Elsevier, New York, NY, 1996.

[27] J.M.M. Peeters, J.P. Boom, M.H.V. Mulder, H.U. Strathmann, Retention measurements of nanofiltration membranes with electrolyte solutions, J. Memb. Sci. 145 (1998) 199–209.

[28] F. Berné, Y. Richard, Water treatment handbook. 6th ed., vol. 1 & 2, Paris: Lavoisier; 1991.